Room-Temperature Indentation Creep of Lead-Free Sn-5%Sb Solder Alloy

A.R. GERANMAYEH[1] and R. MAHMUDI[2,3]

1.—Department of Mechanical Engineering, Azad University, South Tehran Branch, Tehran, Iran. 2.—Department of Metallurgical and Materials Engineering, Faculty of Engineering, University of Tehran, Tehran, Iran. 3.—E-mail: mahmudi@ut.ac.ir

Creep behavior of the lead-free Sn-5%Sb solder alloy was studied by long-time Vickers indentation testing at room temperature. Four different conditions of the material were examined. These were unhomogenized cast (UC), homogenized cast (HC), unhomogenized wrought (UW), and homogenized wrought (HW) conditions. Based on the steady-state power-law creep relationship, the stress exponents were determined through different methods of analysis, and in all cases, the calculated exponents were in good agreement. The stress exponent values of about 5 and 12, depending on the processing route of the material, are very close to those determined by room-temperature conventional creep testing of the same material reported in the literature. For the HW condition, the n value of about 5 together with a very fine grain size of 4.5 μm and a high volume fraction of second-phase particles of 8.6% may suggest that dislocation climb is the creep mechanism. For all other conditions with different grain sizes and second-phase volume fractions, however, the high n value of 12 implies that the operative creep mechanism is dislocation creep, which is independent of grain size.

Key words: Lead-free solder, creep, stress exponent, indentation

INTRODUCTION

Due to the environmental problems of lead-containing solders, it is quite desirable to replace them by lead-free alloys. Tin-antimony alloys are considered as suitable candidates for this purpose. Sn-5%Sb with a near-peritectic composition, a relatively high melting point of 245°C, and a solder-substrate contact angle of about 43° is one of these materials used as solders in electronic packaging.[1,2] Low-cycle fatigue, resulting from differences in the coefficient of thermal expansion between components connected by solder joints, is a prime cause of joint failure in the electronic industry.[3] In these fatigue processes, however, creep mechanisms play an important role because of the high homologous temperatures involved. Furthermore, in some applications, such as optical interconnects, dimensionally stable solders are needed because any creep deformation may result in a device failure.[4] Therefore, the creep study of tin-antimony alloys has received a great deal of attention.[1,2,5–7] The general conclusion is that while antimony atoms in solution have only a minor effect on the creep resistance, alloys with higher concentrations of antimony contain cuboid and whisker-type SnSb precipitates, which provide a significant composite strengthening effect that reduces the creep rate of the material especially at temperatures below 100°C.

Several papers have addressed the possibility of gaining information on creep properties by the use of indentation or long-time hardness tests.[8–12] When a constant load is applied on the surface of a sample with a suitable indenter over a period of time, plastic yield and creep take place as the indenter penetrates the material. The variation in the indentation size, expressed either as a change in diameter (Brinell test) or diagonal length (Vickers test), is monitored with dwell time. Thus, the time-dependent flow behavior of materials can be studied by these simple hardness tests. This can be particularly advantageous when the material is only available as small

(Received November 23, 2004; accepted January 7, 2005)

test pieces or there are some difficulties with the machining of samples made of very soft materials. Therefore, the indentation creep tests, regarded as a quick, simple, and nondestructive procedure to extract information on the mechanical behavior of materials, greatly reduce the effort for sample preparation.[13,14]

The majority of published work on the indentation and impression creep behavior of solder alloys has focused on the eutectic Pb-62.8%Sn alloy.[8,15–18] However, other solder materials such as Pb-9%Sn[19] and more recently Sn-3.5%Ag[20,21] have also been studied by indentation and impression testing techniques. On the other hand, the creep behavior of the lead-free Sn-Sb alloys is mostly studied by conventional creep test and in one case by the automated ball indentation (ABI) method.[1] Thus, the indentation creep of Sn-5%Sb solder has not been studied before and will be attempted in this investigation.

METHODS OF INDENTATION CREEP ANALYSIS

It is generally accepted that the mechanical behavior of metallic materials at homologous temperatures higher than 0.3 can be fairly expressed by the power-law creep in a wide range of strain rates.[22–25] Thus, for steady-state creep, the relationship between the strain rate, $\dot{\varepsilon}$, and the tensile stress, σ, at a constant temperature can be expressed by

$$\dot{\varepsilon} = A\,\sigma^{n} \tag{1}$$

where n is the steady-state stress exponent, defined as $n = \left[\frac{\partial \ln \dot{\varepsilon}}{\partial \ln \sigma}\right]_{\varepsilon}$, and A is a constant.

Mulhearn and Tabor[26] proposed an expression of the following form to acquire the steady-state stress exponent for pure lead at temperatures above $0.6T_m$:

$$-\left(n+\frac{1}{2}\right)\log H_V = \log t + B \tag{2}$$

where H_V is the Vickers number, t is the indentation dwell time, and B is a constant. If hardness is plotted against time on a log-log scale, a straight line with slope $(n + 1/2)^{-1}$ is obtained.

Juhasz et al.[27] carried out tests on a superplastic lead-tin alloy using Vickers tests and obtained the stress exponent (n) in steady-state creep of the following form:

$$n = \left[\frac{\partial \ln \dot{d}}{\partial \ln H_V}\right]_{d} \tag{3}$$

where H_V is the Vickers hardness number, d is the indentation diagonal length, and $\dot{d}$ is the rate of variation in indentation length. This implies that if $\dot{d}$ is plotted against H_V on a double logarithmic scale, a straight line will be obtained, the slope of which is the stress exponent, n.

More recently, Sargent and Ashby[23] carried out hot hardness tests on a wide range of materials and proposed a dimensional analysis for indentation creep. According to their model, the displacement rate of an indenter has been derived as

$$\frac{du}{dt} = \left[\frac{\dot{\varepsilon}_0}{C_2}\left(\sqrt{A}\right)\right]\left[\left(\frac{C_1}{\sigma_0}\right)\left(\frac{P}{A}\right)\right]^{n} \tag{4}$$

where A is the projected area of indentation, C_2 is a constant, $\dot{\varepsilon}_0$ is the rate at a reference stress σ_0, n is the stress exponent, and P is the applied load. For a pyramid indenter, the penetration is proportional to $\sqrt{A}$, i.e.,

$$u = C_3\sqrt{A} \tag{5}$$

Differentiating Eq. 5 with respect to time and substituting into Eq. 4 gives

$$\frac{dA}{dt} = C_4\,\dot{\varepsilon}_0\,A\left(\frac{P}{A}\sigma_0\right)^{n} \tag{6}$$

where C_3 and C_4 are constants. When P is held constant, Eq. 6 can be rewritten as

$$\left(\frac{1}{H_V}\right)\left(\frac{dH_V}{dt}\right) = -C_4\,\dot{\varepsilon}_0\left(\frac{H_V}{\sigma_0}\right)^{n} \tag{7}$$

Sargent and Ashby have derived the following relationship between indentation hardness and dwell time:

$$H_V(t) = \frac{\sigma_0}{\left(nC_4\,\dot{\varepsilon}_0\,t\right)^{\frac{1}{n}}} \tag{8}$$

where $H_V(t)$ is the time-dependent hardness. Hence, from Eq. 8, the slope of a plot of $\ln(H_V)$ against $\ln(t)$ at a constant temperature is $-\frac{1}{n}$. Also, from Eq. 7, a plot of $\ln(H_V)$ versus $\ln\left[-\left(\frac{1}{H_V}\right)\left(\frac{dH_V}{dt}\right)\right]$ at a constant temperature has a slope of n.

To use the Sargent-Ashby analysis, we convert the term $\frac{1}{H_V}.\frac{dH_V}{dt}$ in Eq. 7 to a more measurable quantity. Vickers hardness is given by $H_V = 0.1854F/d^2$ where F is the applied load in N and d is the average diagonal length in mm. Therefore, the relationship between Vickers hardness and applied load can be expressed as

$$0.1854F = d^2 \cdot H_V \tag{9}$$

On the other hand, during the indentation test, the applied load is constant; therefore, differentiating Eq. 9 gives

$$\frac{dH_V}{dt}\cdot d^2 = -2d\,\frac{d(d(t))}{dt}\cdot H_V \tag{10}$$

This equation can be further simplified to the following form:

$$-\frac{dH_V}{dt}.\frac{1}{H_V} = \frac{2\dot{d}}{d} \tag{11}$$

Substituting Eq. 7 into Eq. 4 gives

$$n \log H_V = \log\left(\frac{2\dot{d}}{d}\right) + C \qquad (12)$$

Thus, a plot of $\log\left(\frac{2\dot{d}}{d}\right)$ versus $\log H_v$ at a constant applied load F has a slope of n and the stress exponent can be obtained.

The objective of this paper is to investigate the power-law indentation creep behavior of cast and wrought Sn-5%Sb alloys at room temperature ($T > 0.5T_m$), by measuring the stress exponents for these materials using different methods of analysis for indentation creep.

EXPERIMENTAL PROCEDURE

Materials and Processing

The material used was a Sn-Sb alloy containing 5wt.%Sb. It was prepared from high-purity tin (99.99%) and a Sn-20%Sb master alloy melted in an electrical furnace under inert argon atmosphere, and cast into 120 × 30 × 12-mm slabs. To study the effect of homogenization on the creep behavior of the material, some of the slabs were homogenized for 24 h at 505 K. Some of the homogenized and unhomogenized cast slabs were cut into 2 × 30 × 12-mm slices using an electrodischarge wire cut machine, and some others were rolled to a 83% reduction at room temperature ($T > 0.5T_m$) in order to generate a homogeneous fine-grained material without the initial as-cast structure. Homogenized and unhomogenized conditions are referred to hereafter as "H" and "U," respectively, followed by "C" for the cast and "W" for the wrought materials. Both cast and wrought conditions were studied by optical microscopy to examine the microstructure evolution of the materials. These specimens were polished with 0.25-μm diamond paste, followed by polishing on a microcloth without any abrasive. Etching was carried out using a 2% nitric acid and 98% alcohol solution at room temperature. The structure of the materials was thus revealed and the average grain size was measured by the grain count method in which an average grain size may be obtained from measurements of the number of grains per unit area on a polished surface.[28] X-ray diffraction (XRD) and image analysis were carried out on selected samples for different experimental conditions.

Indentation Creep Tests

The polished specimens were tested in a Vickers hardness tester where the applied load and testing time were the only variables. In the Vickers test, a diamond pyramid with square base is used and the Vickers hardness number is given by $H_V = 0.185F/d^2$, where F is the applied load in N and d is the average diagonal length in millimeters. Indentation creep measurements were made on each sample using loads of 20 N, 30 N, 50 N, and 100 N for dwell times up to 120 min. Each reading was an average of at least five separate measurements taken at random places on the surface of the specimens. All of the indentations were at least 5 mm away from the edges and from other indentations.

RESULTS AND DISCUSSION

Preliminary study of room-temperature creep of the material was carried out by testing the cast alloy under a constant load for different times. It was observed that the indentation length becomes larger with increasing loading time. The indentation creep data were measured at room temperature under constant loads of 20 N, 30 N, 50 N, and 100 N. The results are shown in Figs. 1 and 2, where the indentation length is plotted against time. It can be seen from these figures that the indentation length increases with the loading time and the applied load. It can also be inferred that in all four conditions of the material, the shape of the indentation curve is similar to that of an ordinary creep curve. The first stage of the curve records an increase in the concerned variable with time, with a decreasing rate, followed by a steady-state region, where indentation sizes increase linearly with time. As the hardness test is actually a compression test, fracture of the specimen does not occur and hence it is obviously not possible to record a third stage of the curve as opposed to what happens in an ordinary creep test. Figures 1 and 2 also indicate that various conditions of the material exhibit different indentation creep behavior. It

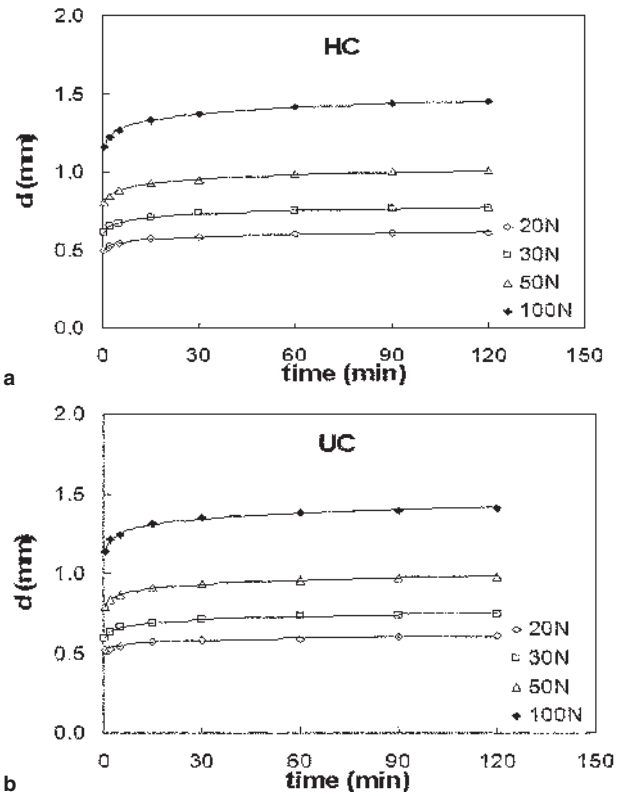

Fig. 1. Indentation creep curves at different loads for the cast materials in the (a) homogenized and (b) unhomogenized conditions.

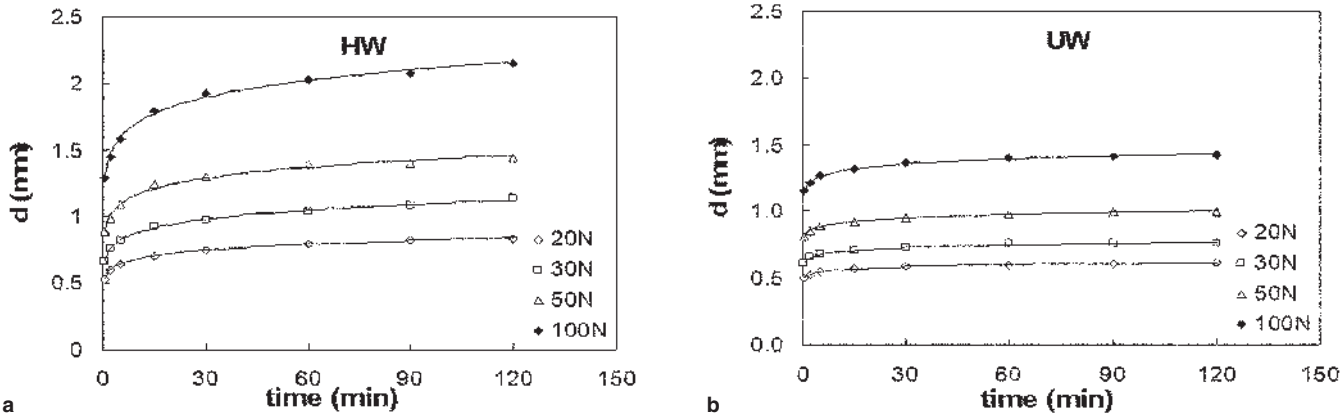

Fig. 2. Indentation creep curves at different loads for the wrought materials in the (a) homogenized and (b) unhomogenized conditions.

can be depicted from these figures that the level of indentation curves and their slopes in the steady-state region are higher for the homogenized wrought (HW) condition. Other conditions, however, show very similar behaviors in terms of the level and slope of the indentation curves, implying that while indentation creep occurs more readily in the HW condition, there is not much difference in indentation creep behavior of UW, HC and UC conditions.

The three aforementioned methods of Mulhearn-Tabor,[26] Juhasz et al.,[27] and Sargent-Ashby[23] have been applied to the indentation data of the materials to obtain the steady-state creep exponents. According to the Mulhearn-Tabor relationship, Eq. 2, if hardness is plotted against time on a double logarithmic scale, a straight line with slope $-(n + 1/2)^{-1}$ is obtained. This has been represented in Figs. 3 and 4 for all materials and testing loads. Using the Juhasz et al. method, Eq. 3, the rate of diagonal variation is plotted against the Vickers hardness number on a double logarithmic scale in Figs. 5 and 6. A straight line with a slope of n results for

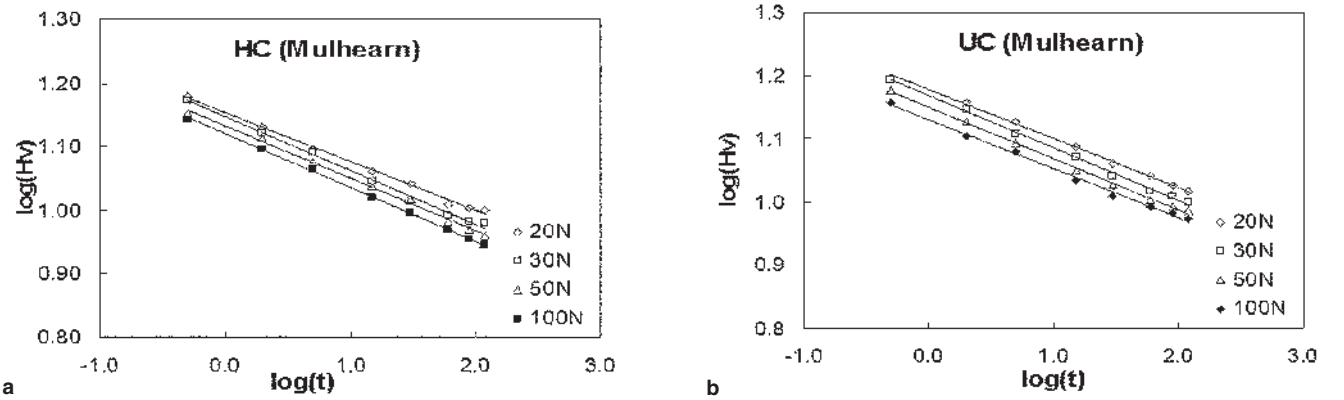

Fig. 3. Derivation of stress exponent for the (a) homogenized cast and (b) unhomogenized cast conditions by the Mulhearn-Tabor indentation method.

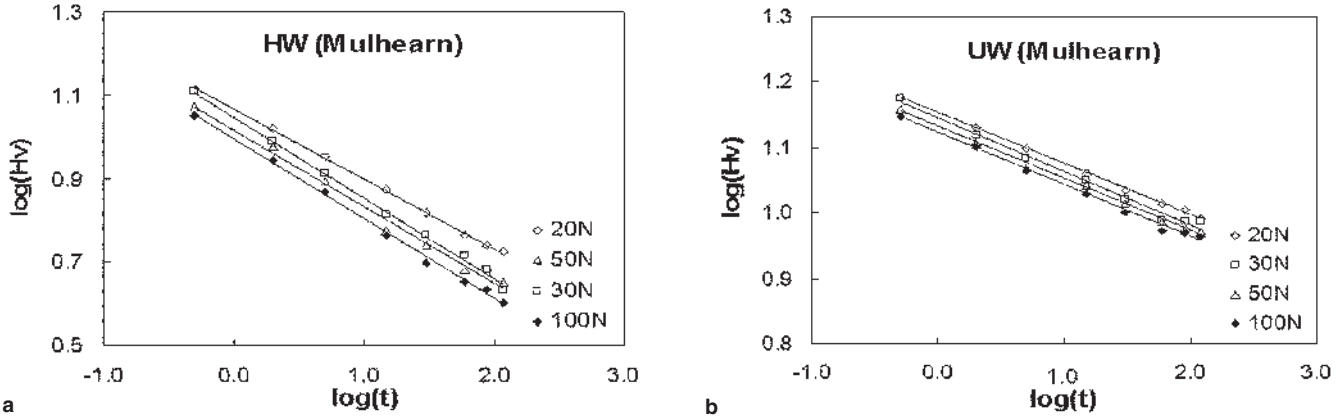

Fig. 4. Derivation of stress exponent for the (a) homogenized wrought and (b) unhomogenized wrought conditions by the Mulhearn-Tabor indentation method.

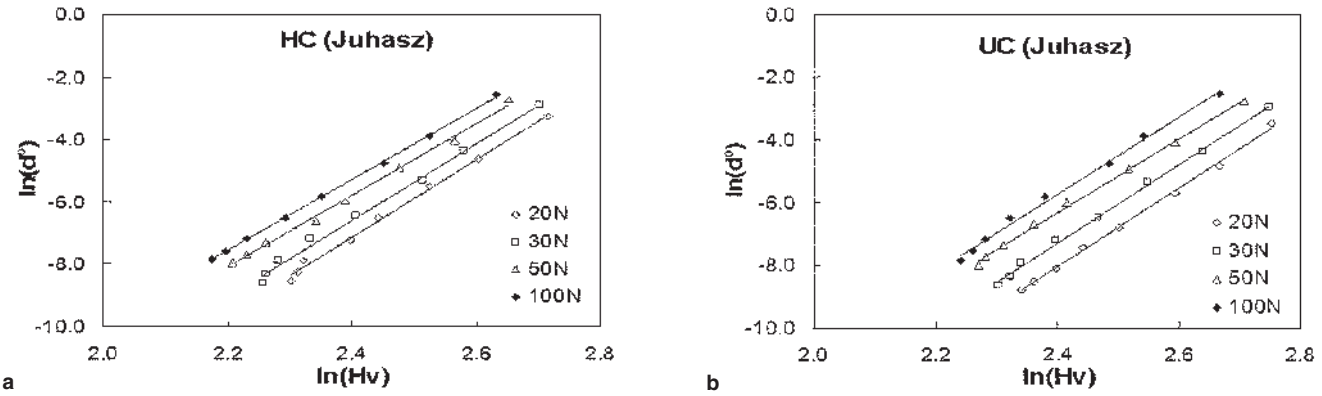

Fig. 5. Derivation of stress exponent for the (a) homogenized cast and (b) unhomogenized cast conditions by the Juhasz et al. indentation method.

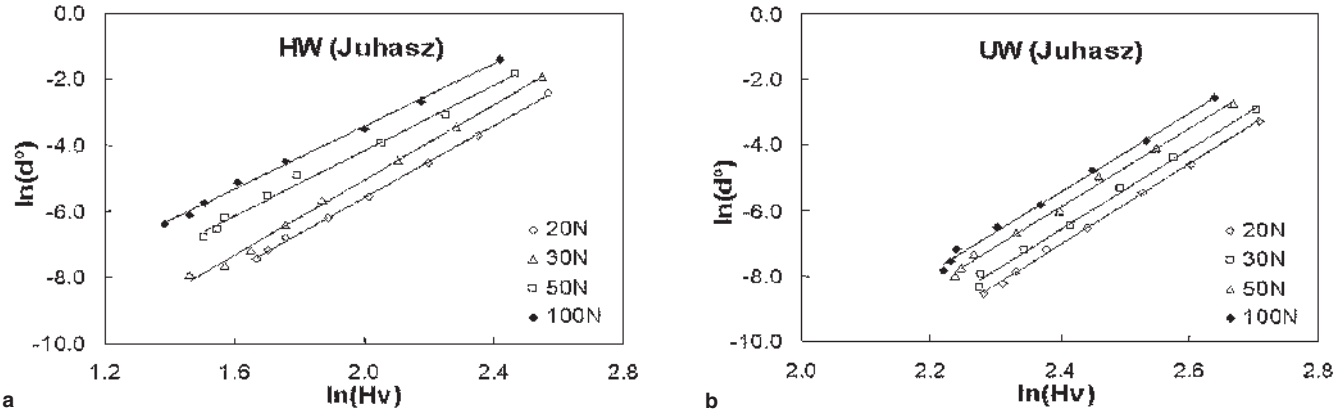

Fig. 6. Derivation of stress exponent for the (a) homogenized wrought and (b) unhomogenized wrought conditions by the Juhasz et al. indentation method.

each alloy and load. The rate of the diagonal variation has been obtained by differentiation of the curves in Figs. 1 and 2. Applying the Sargent-Ashby model, the stress exponent can be obtained from a plot of $\log\left(\frac{2\dot{d}}{d}\right)$ versus $\log H_V$ having a slope of n. This is illustrated in Figs. 7 and 8 for all materials and testing loads.

The interesting feature of all three methods is that for each material the fitted lines are almost parallel, implying that the stress exponent is independent of the applied load. The stress exponent values obtained for each alloy via each of the above-mentioned approaches at different loads are represented in Table I. These exponents are in the range of 11.6–13.1, 11.3–12.9, 11.8–13.2, and 4.7–6.2 for UC, HC, UW, and HW conditions, respectively. It is worth noting that the results of conventional creep tests on a cast and aged Sn-5.8%Sb alloy at room temperature are indicative of n values of 11.6 and 5.3 at high and low stresses, respectively.[3] Other

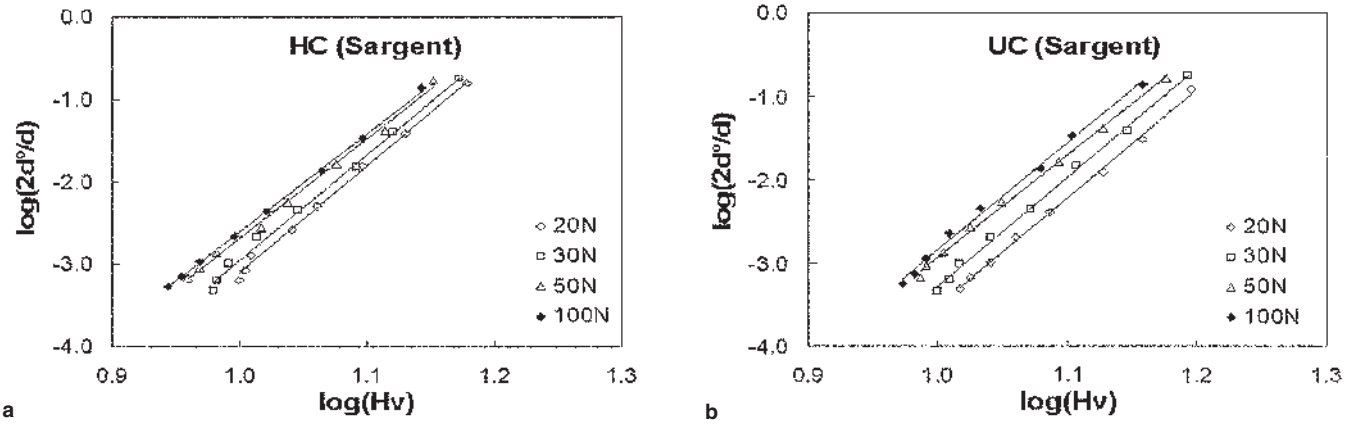

Fig. 7. Derivation of stress exponent for the (a) homogenized cast and (b) unhomogenized cast conditions by the Sargent-Ashby indentation method.

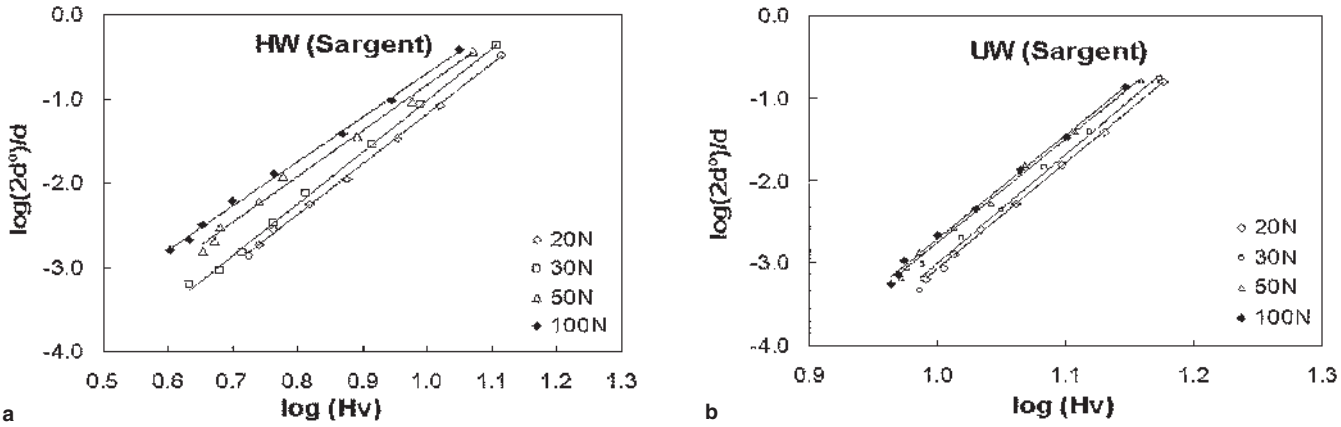

Fig. 8. Derivation of the stress exponent for the (a) homogenized wrought and (b) unhomogenized wrought conditions by the Sargent-Ashby indentation method.

similar results obtained in the conventional and automated ball indentation ABI creep testing of rolled Sn-5%Sb sheets have yielded n values of about 5 at room temperature.[1]

In the present work, the stress exponents calculated by different approaches are in good agreement with each other, indicating the similarity of the derivation methods. A useful finding is that the relationship proposed by Mulhearn-Tabor[26] is applicable to hardness tests with Vickers indenter, although this relationship was originally developed for a spherical indenter. According to the power-law creep, a decrease in stress exponent would result in an increase in creep rate due to a decrease in yield strength.[27,29] Therefore, the HW material with significantly lower n values is less resistant to indentation creep compared to the other conditions, which all exhibited almost similar behavior, as shown by their n values of about 12. The same result can also be extracted from the indentation curves shown in Figs. 1 and 2.

The microstructures of the cast and wrought materials are shown in Figs. 9 and 10, respectively. It is observed that the UC condition has a dendritic structure with a dendrite arm spacing (DAS) of about 35 μm. The HC material, however, has a rather coarse equiaxed grain structure with an average grain size of about 280 μm. This implies that the long-time homogenization treatment has totally removed the dendritic structure, resulting in a recrystallized structure with little intermetallic particles at the grain boundaries. Both of the wrought conditions have equiaxed grain structures with different grain sizes of 60 μm and 4.5 μm for the UW and HW conditions, respectively. It seems that homogenization of the cast material followed

Table I. Materials Characteristics and the Stress Exponents (n-Values) Derived from Different Indentation Methods

			Stress Exponent (n)			
			Indentation Tests			
Condition	Grain Size (μm)	Particle Volume Fraction (%)	Load (N)	Mulhearn-Tabor	Juhasz et al.	Sargent-Ashby
UC	35*	0.23	20	12.5	12.6	12.9
			30	11.6	12.6	13.1
			50	11.8	11.8	12.2
			100	12.3	12.3	12.8
HC	280	0.79	20	12.5	12.4	12.9
			30	11.3	12.3	12.7
			50	11.5	11.5	12.0
			100	11.3	11.4	11.9
UW	60	1.0	20	12.4	12.4	12.8
			30	11.8	12.3	13.2
			50	12.1	12.0	12.5
			100	12.1	12.1	12.6
HW	4.5	8.6	20	5.5	5.5	6.0
			30	5.7	5.7	6.2
			50	4.9	4.9	5.4
			100	4.7	4.7	5.2

* DAS

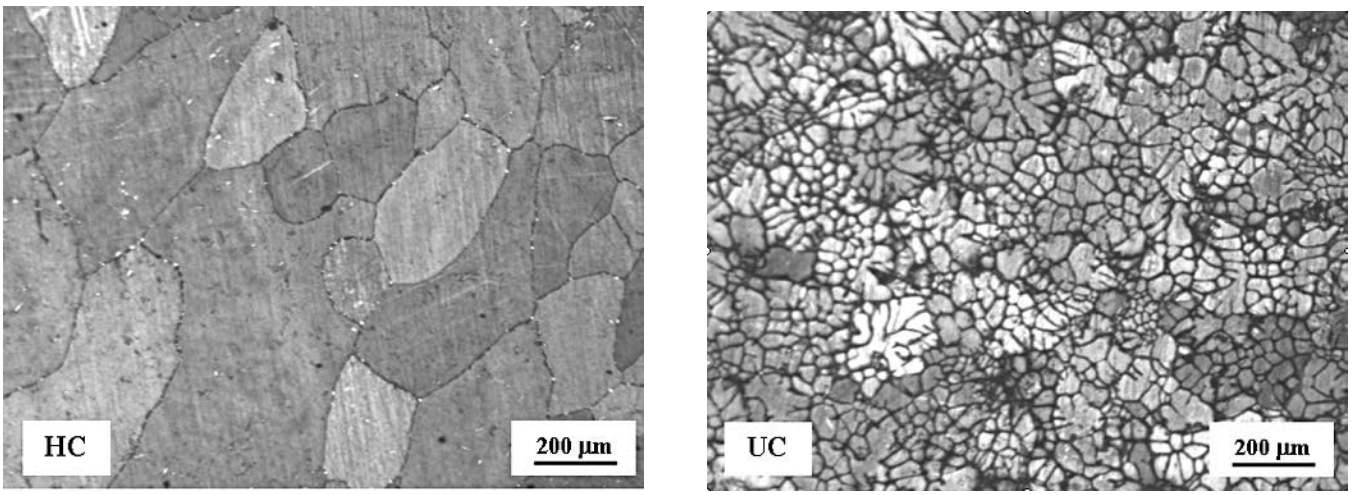

a b

Fig. 9. Optical microstructures of the cast materials in the (a) homogenized and (b) unhomogenized conditions.

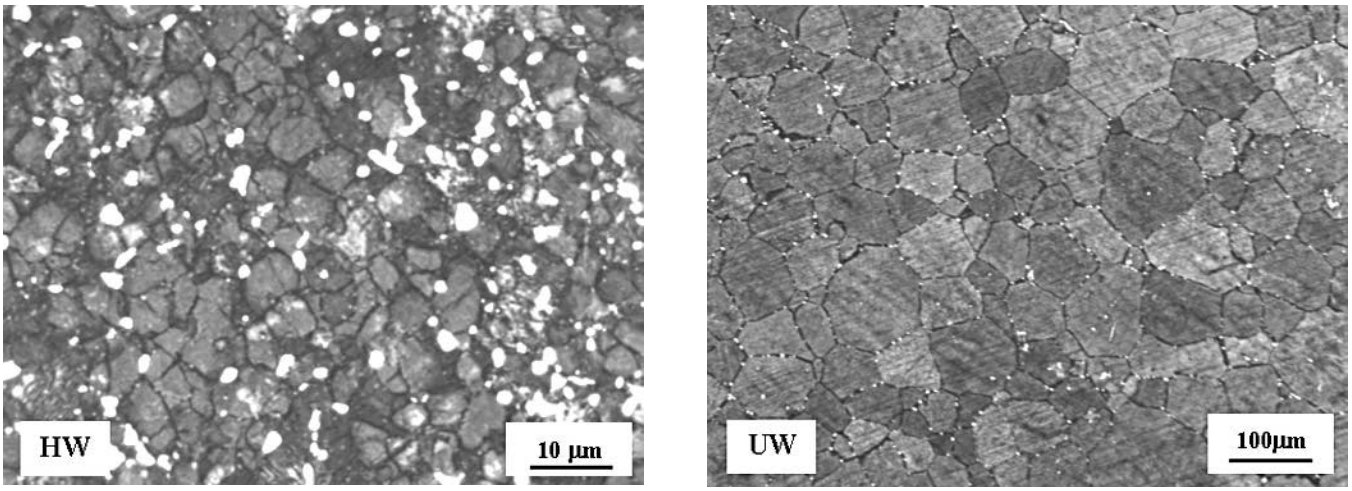

a b

Fig. 10. Optical microstructures of the wrought materials in the (a) homogenized and (b) unhomogenized conditions.

by cold rolling provides sufficient driving force for precipitation of the second-phase particles and a complete recrystallization of the material. The volume fractions of the intermetallic second-phase particles, determined by the image analysis, are also included in Table I. The high volume fraction of the particles in the HW condition is in sharp contrast with those of the other conditions.

The XRD analysis was employed in order to identify the type of the precipitated phases. Figure 11 shows the XRD pattern of the wrought materials in the unhomogenized and homogenized conditions. It is observed that the Sn matrix and the precipitated SnSb particles are the only constituents of the material. However, the higher amount of the second phase in the HW condition has resulted in more distinct peaks of the SnSb phase in its diffraction pattern. This is also confirmed by the measured high 8.6% volume fraction of the SnSb particles as compared to the low volume fraction of only 1.0% in the UW material.

The stress exponent values have been frequently used to identify the mechanisms controlling the deformation process. However, it should be cautioned that making mere comparisons of the stress exponents, without additional information on activation energies, does not provide sufficient information to draw insightful comparisons on creep mechanisms of materials. At best, creep stress exponents can only help to narrow the field among many theoretical possibilities. In the present investigation, although the structure of the UC, HC, and UW conditions are totally different in terms of grain size and second-phase volume fraction, they all exhibit the same stress exponent of 12. This high n value implies that the operative creep mechanism is dislocation creep, which is independent of grain size. Furthermore, the particles are all on the grain boundaries and thus have little impact on dislocation creep. Therefore, the insensitivity of the n value to grain size and particle volume fraction is related to the creep regime studied, and does not represent any fundamental

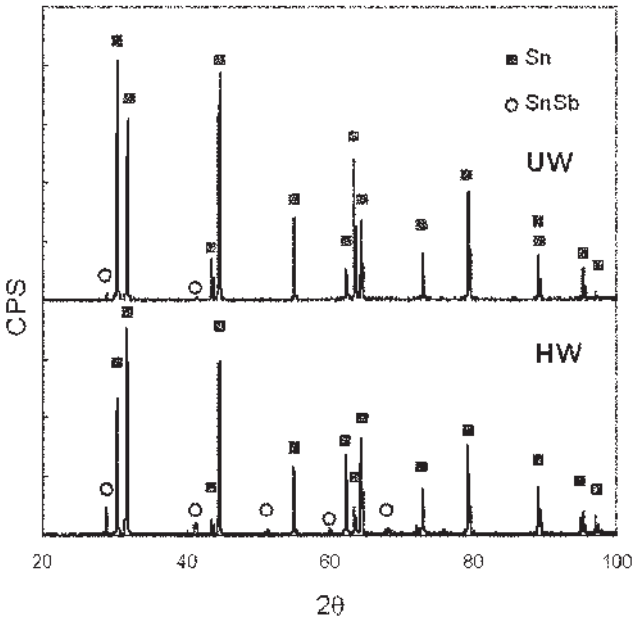

Fig. 11. XRD patterns of the UW and the HW conditions.

characteristic of the material. For the HW condition, however, the n value of about 5 together with the very fine grain structure and a high volume fraction of second-phase particles suggest that dislocation climb could be the creep mechanism.

CONCLUSIONS

- It is experimentally shown that an indentation creep process occurs in Sn-5%Sb alloys at room temperature. In all conditions, the stress exponent values are independent of the loading conditions.
- The data analyses have also shown that the simple theory, based on the steady-state power-law creep equation, has the capacity to describe the indentation creep data satisfactorily. The indentation creep test is demonstrated to be capable of evaluating creep behavior of materials using small specimens.
- The stress exponents calculated from different methods of analysis are in good agreement with each other. The stress exponents obtained from different approaches were found to be about 5 for the homogenized wrought material and about 12 for all other conditions of the alloy. This implies that cast alloys show typically higher resistance to indentation creep compared to the wrought alloy in the homogenized condition.
- According to the measured stress exponents, dislocation climb might be the dominant creep mechanism in the fine-grained alloy containing a high volume fraction of precipitated phase and the dislocation creep could be the operating creep mechanism in all other conditions having a rather coarse grain size and a low volume fraction of second-phase particles.

REFERENCES

1. K.L. Murty, F.M. Haggag, and R.K. Mahidhara, *J. Electron. Mater.* 26, 839 (1997).
2. P.T. Vianco and D.R. Frear, *JOM* 45(7), 14 (1993).
3. R.J. McCabe and M.E. Fine, *Metall. Mater. Trans. A* 33A, 1531 (2002).
4. H. Mavoori, *JOM* 52(6), 29 (2000).
5. M.H.N. Beshaie, S.K. Habib, A.M. Yassein, G. Saad, and M.H. Hasab El-Naby, *Cryst. Res. Technol.* 34, 119 (1999).
6. R.J. McCabe and M.E. Fine, *J. Electron. Mater.* 31, 1276 (2002).
7. N. Wade, K. Wu, J. Kuni, S. Yamada, and K. Miyahara, *J. Electron. Mater.* 30, 1228 (2001).
8. M. Fujiwara and M. Otsuka, *Mater. Sci. Eng.* A319–A321, 929 (2001).
9. R. Mahmudi, R. Roumina, and B. Raeisinia, *Mater. Sci. Eng.* A382, 15 (2004).
10. T.R.G. Kutty, T. Jarvis, and C. Ganguly, *J. Nucl. Mater.* 246, 189 (1997).
11. R. Roumina, B. Raeisinia, and R. Mahmudi, *Scripta Mater.* 51, 497 (2004).
12. T.R.G. Kutty, C. Ganguly, and D.H. Sastry, *Scripta Mater.* 34, 1833 (1996).
13. A. De La Torre, P. Adeva, and M. Aballe, *J. Mater. Sci.* 26, 4351 (1991).
14. G. Sharma, R.V. Ramanujan, T.R.G. Kutty, and G.P. Tiwari, *Mater. Sci. Eng.* A278, 106 (2000).
15. F. Yang and J.C.M. Li, *Mater. Sci. Eng,* A201, 40 (1995).
16. A. Juhasz, P. Tasnadi, P. Szasvari, and I. Kovacs, *J. Mater. Sci.* 21, 3278 (1986).
17. M.J. Mayo and W.D. Nix, *Acta Metall.* 36, 2183 (1988).
18. K.L. Murty, *Mater. Sci. Eng.* A14, 169 (1974).
19. T.T. Fang, R.R. Cola, and K.L. Murty, *Metall. Trans. A* 17A, 1447 (1986).
20. S. Devaki Rani and G.S. Murthy, *Mater. Sci. Technol.* 20, 403 (2004).
21. I. Dutta, C. Park, and S. Choi, *Mater. Sci. Eng.* A379, 401 (2004).
22. G. Cseh, N.Q. Chinh. P. Tasnadi, and A. Juhasz, *J. Mater. Sci.* 32, 5107 (1997).
23. P.M. Sargent and M.F. Ashby, *Mater. Sci. Technol.* 8, 594 (1992).
24. B.N. Lucas and W.C. Oliver, *Metall. Mater. Trans. A* 30A, 601 (1999).
25. T.G. Langdon, *Mater. Sci. Eng.* A283, 266 (2000).
26. T.O. Mulhearn and D. Tabor, *J. Inst. Met.* 89, 7 (1960).
27. A. Juhasz, P. Tasnadi, and I. Kovacs, *J. Mater. Sci. Lett.* 5, 35 (1986).
28. G.E. Dieter, *Mechanical Metallurgy,* 3rd ed (New York: McGraw-Hill, 1986), pp. 191–192.
29. G. Cseh, J. Bar, H.J. Gudladt, J. Lendvai, and A. Juhasz, *Mater. Sci. Eng.* A272, 145 (1999).